

The simultaneous detection of 22- and 321-GHz H₂O maser emission towards the symbiotic Mira R Aquarii

R. J. Ivison¹, J. A. Yates² and P. J. Hall³

¹ *Institute for Astronomy, University of Edinburgh, Blackford Hill, Edinburgh EH9 3HJ*

² *Division of Physics and Astronomy, Dept of Physical Sciences, University of Hertfordshire, College Lane, Hatfield AL10 9AB*

³ *Australia National Telescope Facility, CSIRO, PO Box 76, Epping, NSW 2121, Australia*

Accepted ... Received ... in original form 1997 June 24

ABSTRACT

We report high spatial and spectral resolution measurements of masers towards R Aqr and H1–36, both of which are examples of the sub-class of symbiotic stars that contain a long-period Mira-type variable. Our observations have resulted in the first detection of 321-GHz H₂O maser action towards a symbiotic Mira — R Aqr. Comparison with simultaneous 22-GHz H₂O maser data suggests the masers do not have the same properties as those in the circumstellar envelopes of field Miras. R Aqr’s 22-/321-GHz peak flux density and luminosity ratios are low, as is the line-width ratio. Continuum and spectral-line maps indicate that the 22-GHz maser and free-free emission are aligned. Three mechanisms can reproduce the data with varying degrees of success. All three lead naturally to normal levels of maser emission in SiO and 321-GHz H₂O and anomalously weak OH and 22-GHz H₂O masers. In the most convincing model, UV radiation and a fast wind from the companion remove the Mira’s envelope of dusty, molecular gas, leaving a relatively small cavity of dense, neutral material within a large, ionized nebula. Excitation temperatures suggest that 321-GHz masers are normally excited close to the Mira whilst 22-GHz masers are more remote; in R Aqr, therefore, the 22-GHz masers do not form under optimum conditions. Instead, we see weak and narrow lines that form closer to the Mira, consistent with our high-resolution maps.

Key words: masers — binaries: symbiotic — stars: individual: R Aqr, H1–36 Arae

1 INTRODUCTION

R Aqr is the closest known symbiotic Mira. It is a binary system in which a late-type, long-period variable giant loses matter to a post-AGB dwarf. Existing models have failed to account convincingly for many of the simplest features of the R Aqr system: the binary period, the method of mass transfer, the nature of the hot, companion star and its outburst mechanism. Still less is known about the more unusual phenomenon on display: the transient jet-like prominence (Wallerstein & Greenstein 1980; Sopka et al. 1982) and the arcmin-scale nebulae (Solf & Ulrich 1985).

Various studies have shown that the molecular emission lines of symbiotic stars are very different from those expected from isolated Miras. For example, Bowers & Hagen (1984) stated that 75 per cent of Miras in the solar neighbourhood have 22-GHz H₂O maser emission, whereas Seauquist, Ivison & Hall (1995 — SIH95) reported that only two of the twenty-five known Mira-type symbiotic stars support 22-GHz H₂O masers. R Aqr and H1–36 are the unusual duo. The reasons why these systems are peculiar are not well understood, but it seems likely that it is because of the rel-

atively large size of the binary orbit in the case of H1–36, and because of the low luminosity of the hot companion star in the case of R Aqr (compared with other symbiotic objects in the samples observed by SIH95 and Schwarz et al. 1995).

R Aqr and H1–36 also harbour amongst the brightest known SiO masers. R Aqr has been detected in the 43-GHz $J = 1 - 0$ lines of both the $v = 1$ and $v = 2$ states (Martinez et al. 1988), with SiO fluxes at 43 GHz averaging around 100 Jy over several pulsational periods, with the flux and velocity of individual features varying considerably from one period to the next. It has also been detected in the $v = 1$, $J = 2 - 1$ transition at 86 GHz (Hollis et al. 1990). Schwarz et al. show that the peak of the 86-GHz emission averages about 200 Jy, but varies with stellar phase and between different periods in both flux and velocity (like the 43-GHz emission). Finally, R Aqr is also one of a handful of systems to display the $J = 7 - 6$ SiO transition (Gray et al. 1995).

In a recent survey of twenty-two circumstellar envelope 22-GHz H₂O maser sources, Yates, Cohen and Hills (1995) showed that 70 per cent had observable sub-mm H₂O emission. The velocity extent of 321-GHz maser emission was

Table 1. Parameters for four epochs of 22-GHz observations of R Aqr.

UT Date	Array configuration	Synthesized beam size and PA	Dominant peak velocity (km s ⁻¹)	Position (B1950)	
				$\alpha(23^{\text{h}}41')$	$\delta(-15^{\circ}33')$
1993 May 16	CnB	1.8'' \times 0.6'', 124°	-26.6 \pm 0.2	14.27 \pm 0 ^s .02	43.30 \pm 0''.15
1994 May 20	BnA	0.2'' \times 0.1'', 55°	-26.8 \pm 0.2	14.27 \pm 0 ^s .01	43.35 \pm 0''.03
1995 June 8	D	4.3'' \times 2.6'', 154°	-24.7 \pm 0.2	14.26 \pm 0 ^s .03	43.19 \pm 0''.60

less than that at 22-GHz and the 22-GHz peak flux density was typically twice that at 321-GHz.

Here, we report the first detection of the $J = 10_{29} - 9_{36}$ ortho 321-GHz H₂O maser transition towards a symbiotic Mira system. Poor observing conditions prevented any attempt to detect the para $J = 5_{15} - 4_{22}$ 325-GHz H₂O maser transition which sits in a deep atmospheric absorption trough. Our sub-mm observations were performed using the James Clerk Maxwell Telescope, whilst observations of the $J = 6_{16} - 5_{23}$ 22-GHz H₂O maser transition were obtained contemporaneously using the Very Large Array.

2 OBSERVATIONS

2.1 James Clerk Maxwell Telescope

The JCMT observations were carried out at two epochs. A liquid-helium-cooled, single-channel SIS mixer receiver, B3i, was used, with a digital autocorrelation spectrometer backend providing a bandwidth of 250 MHz and a channel spacing of 0.156 MHz. The rest frequency adopted for the H₂O $J = 10_{29} - 9_{36}$ transition was 321.22564 GHz, with velocities of -25.0 and -125.0 km s⁻¹ relative to the LSR for R Aqr and H1-36, respectively.

During 1994 May 01, observations were hampered by weather conditions unsuited to observing near the 325-GHz atmospheric water absorption feature — the opacity at 230 GHz was \sim 0.1, giving a 321-GHz system temperature of around 1500 K. We integrated for 1 hr, achieving a 3- σ upper limit on the integrated line flux of 13.8 Jy km s⁻¹.

At the second epoch, 1995 June 05, T_{sys} was \sim 1000 K. After integrating for 5.25 hr (exclusive of overheads such as the time spent nodding the telescope to alternate the signal and reference beams), we obtained a detection of the 321-GHz transition towards R Aqr.

2.2 Very Large Array

Including data reported by Ivison, Seaquist & Hall (1994), interferometric observations at 22 GHz have been carried out using the VLA on four occasions. Here, we describe the latter three epochs.

The telescope was in the A configuration during 1994 May 01-02 when data were obtained for H1-36 and R Aqr covering the 1612- and 1667-MHz OH lines simultaneously with two IF pairs (for H1-36: 195-kHz bandwidth, with 0.28-km s⁻¹ channel separation, for 150 min; for R Aqr: 781-kHz bandwidth, with 1.13-km s⁻¹ channel separation, for 120 min). Data was also obtained for H1-36 covering the 22-GHz H₂O line (6.25-MHz bandwidth, with 1.32-km s⁻¹ channel separation, for 45 min). The H1-36 data were phase

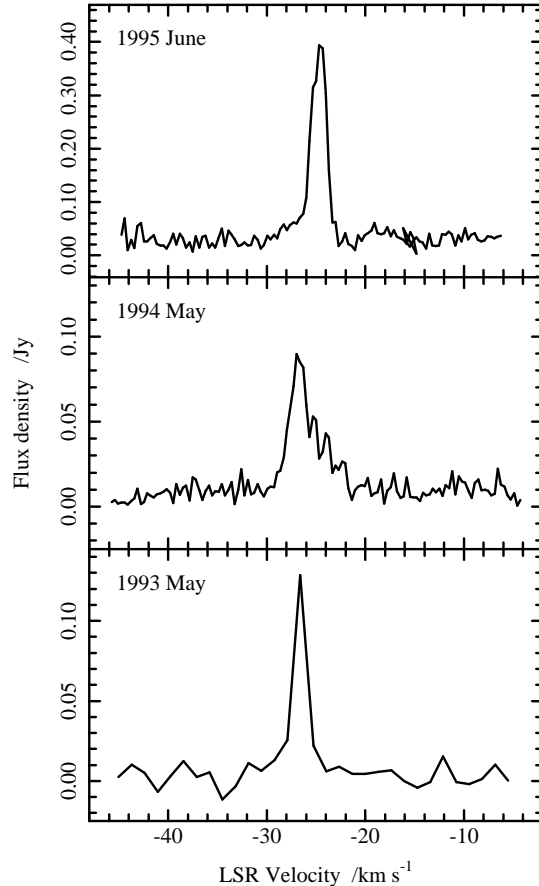


Figure 1. The 22-GHz spectra observed towards R Aqr using the VLA during 1993 May (lower, from Ivison et al. 1994), 1994 May (middle) and 1995 June (upper). Pulsational phases, where $\phi = 0.00$ corresponds to maximum visual light, are $\phi = 0.33, 0.28$ and 0.27 (Chinarova, Andronov & Schweitzer 1996). Improved velocity resolution is apparent in the upper panels.

referenced against 1748–253 and 1741–312 at the low and high frequencies, respectively, whilst the R Aqr data were referenced against 2345–167.

During 1994 May 20, the VLA was used in BnA configuration (i.e. B configuration, with some long N-S baselines). Data were obtained for R Aqr covering the 22-GHz H₂O line (3.125-MHz bandwidth, with 0.33-km s⁻¹ channel separation, for 140 min). A 22-GHz continuum map of R Aqr, with 100-MHz bandwidth, was also obtained.

Our final set of VLA observations were performed, using the D configuration, during 1995 June 08 and were contemporaneous with the JCMT measurements described earlier. Data were obtained covering the 22-GHz H₂O line for both

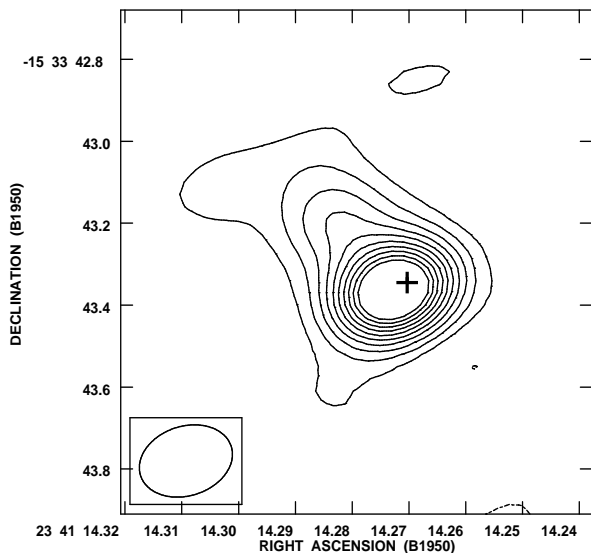


Figure 2. BnA-configuration continuum map of R Aqr at 22 GHz. The map is marked with the position of the 22-GHz H₂O maser and a representation of the restoring beam. The peak flux density is 12.5 mJy beam⁻¹. Contours are plotted at integer values of the 3- σ level (0.85 mJy beam⁻¹). See Ivison et al. (1995a) for a line-free map extracted from the 1665- and 1667-MHz OH data cubes with the position of the 22-GHz H₂O maser marked.

H1–36 and R Aqr (1 hr each, after overheads) with the same bandwidths and channel separations as used in 1994 May.

For all the VLA observations, absolute flux calibration was performed using 0134+329 and 1328+307.

3 OBSERVATIONS OF R AQUARI

3.1 The H₂O masers

Fig. 1 shows all the observations of R Aqr obtained so far with the VLA at 22 GHz. During our initial maser-line survey (reported by Ivison et al. 1994; SIH95), a relatively poor velocity resolution was employed, both to improve our sensitivity to weak lines and to maximise velocity coverage. At subsequent epochs we used narrower channels, which is apparent from the improved velocity resolution of spectra in the upper panels of Fig. 1.

The 22-GHz H₂O line from R Aqr shows temporal variations similar to those seen in its SiO maser lines (Gray et al. 1998). The full velocity width of the 22-GHz H₂O line (8 km s⁻¹) is also the same as that of the 86-GHz $v = 1, J = 2 - 1$ SiO line observed by Schwarz et al. (1995), confirming the speculation of Ivison et al. (1994).

In terms of its position, the H₂O maser is coincident with the centroid of the 22-GHz continuum emission (Fig. 2) (< 50 milliarcseconds, or < 11 au for a distance of 220 pc — van Belle et al. 1996). These data were obtained contemporaneously. During 1994 May, the full velocity extent of 8 km s⁻¹ and the presence of several spectral features suggests that the 22-GHz maser region of R Aqr is complex and made up of several discrete masing clumps. The 0.22×0.11 mas² restoring beam did not resolve any structure, but it does allow us to confirm that the emission mechanism is definitely non-thermal, since $T_b > 12,000$ K.

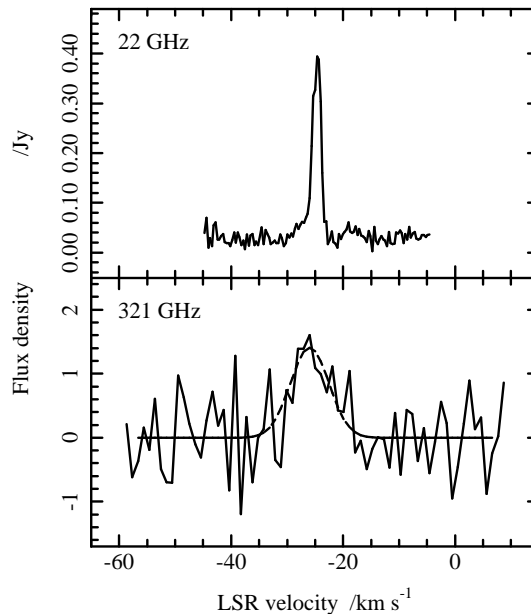


Figure 3. The 22-GHz (upper) and 321-GHz (lower) spectra observed towards R Aqr during 1995 June ($\phi = 0.27$). The 321-GHz data from JCMT have been fitted with a Gaussian profile and are shown after subtraction of a 2nd-order polynomial to the baseline.

At the other two epochs, there was one dominant peak. The velocities of the dominant line peaks during 1993 and 1994 were separated by only 0.2 km s⁻¹, but a 2.1-km s⁻¹ redward shift is evident in the 1995 data. The full profile width is similar at all three epochs, always covering the -22 to -30 km s⁻¹ v_{lsr} interval.

Fig. 3 shows the 22- and 321-GHz spectra obtained during 1995 June for R Aqr. The 321-GHz spectrum is noisy, so it would be a mistake to draw too many conclusions from the line profile or width. The best Gaussian fit to the data yields a FWHM line width of 8 ± 2 km s⁻¹ with a central velocity of -26 ± 1 km s⁻¹ (slightly blueward and broader than the dominant 22-GHz line peak — see below). The integrated flux density is 10.5 ± 2.5 Jy km s⁻¹ and the corresponding photon luminosity is $(3.06 \pm 0.73) \times 10^{41}$ s⁻¹.

The upper plot of Fig. 3 shows the contemporaneous 22-GHz spectrum. As with all our VLA data, the line emission stretches from -22 to -30 km s⁻¹; the dominant peak (0.37 Jy after subtracting off the free-free continuum contribution) is at $v_{\text{lsr}} = -24.7$ km s⁻¹; its FWHM is around 1.8 ± 0.1 km s⁻¹ whilst the integrated flux density of the entire profile, including the pedestal, is 0.73 ± 0.05 Jy km s⁻¹ or $(6.4 \pm 0.4) \times 10^{40}$ photon s⁻¹.

3.2 Comparison with the H₂O masers of field Miras

The recent survey of the profile characteristics of 22- and 321-GHz maser emission from twenty field Miras (Yates et al. 1995) gave a mean ratio of 2.2 for the peak flux densities of the 22- and 321-GHz lines and a mean luminosity ratio of 1.5. There was no apparent correlation between these ratios and the mass-loss rate or the *IRAS* colours, though the line luminosities did correlate with both of these parameters.

For R Aqr we measured a peak flux density ratio of 0.24 ± 0.05 and a photon luminosity ratio of 0.21 ± 0.05 . These lie at the lowest bound of the values observed by Yates et al. (1995). The only objects in the Yates et al. sample that rival these ratios are o Ceti, U Her, R Leo and R Cas; the former is mildly symbiotic – a wind-accreting companion star is separated from the Mira by around 80 au (Karovska, Nisenson & Beletic 1993); all four have relatively low mass-loss rates. R Aqr also has a very low mass-loss rate ($0.06 \times 10^{-6} M_{\odot} \text{ yr}^{-1}$, Seaquist, Krogulec & Taylor 1993).

As was mentioned earlier, Yates et al. (1995) found no correlation between the 22-/321-GHz maser-line photon luminosity ratio and the mass-loss rate for a sample of 13. We have re-analysed the data presented by Yates et al., supplementing them with the result for R Aqr and treating upper and lower limits for the 22-/321-GHz maser-line photon luminosity ratio as though they were detections (the effect of which is to underestimate the degree of correlation, since the systems with low mass-loss rates are those with upper limits and the systems with high mass-loss rates are those with lower limits). With a sample of 19, the resulting correlation coefficient is 0.66, indicating a 99.8 per cent probability that the 22-/321-GHz maser-line ratio varies systematically with the mass-loss rate such that $\log_{10}(L_{22}/L_{321}) = 0.32 + 0.88 \log_{10}(\dot{M}/10^{-6} M_{\odot} \text{ yr}^{-1})$. This would be expected if the maser transitions are inverted at different distances from the central star and a similar trend was tentatively reported by Menten & Melnick (1991).

3.3 The OH lines: upper limits

1612- and 1667-MHz spectra of R Aqr were obtained using the VLA during 1994 June. The 2-hr integration resulted in a substantially lower noise level than that achieved by Ivison et al. (1994); still, neither of the OH lines were detected. The noise level (in a region covering $v_{\text{lsr}} = -96$ to $+46 \text{ km s}^{-1}$) was 2.7 mJy for both spectra (with 1.1-km s^{-1} channels).

If the line tentatively identified by Ivison et al. (1994) at -14 km s^{-1} were a real feature (and OH masers are usually variable on much larger timescales than masers that form closer to the LPV) then we would have detected it at the $\sim 30\text{-}\sigma$ level. Our limit on the integrated flux (assuming a line width of 8.6 km s^{-1}) is $S(3\sigma) < 0.025 \text{ Jy km s}^{-1}$, or $< 1.38 \times 10^{-24} \text{ W m}^{-2}$, and we conclude that the feature described by Ivison et al. (1994) was spurious.

4 OBSERVATIONS OF H1–36

Fig. 4 shows the OH and H₂O spectra of H1–36 obtained during 1994 May. Both the spatial and the velocity resolution were better than those obtained by Ivison et al. (1994) and SIH95 during the survey-style observations, allowing us to rule out a thermal origin for the OH and H₂O line emission ($T_{\text{b}} > 9 \times 10^3$ and $3 \times 10^3 \text{ K}$, respectively). Despite this, the longer integration times reported here meant that the noise values in the OH and H₂O spectra were several times lower than in our 1993 spectra (see Table 2).

The 1612-MHz OH line centroid ($v_{\text{lsr}} = -124.5 \pm 1.0 \text{ km s}^{-1}$) is displaced by -5.5 km s^{-1} from the mainline centroid, though a faint red wing stretches to the centre of the mainline. The full widths are $\sim 8 \text{ km s}^{-1}$ for both of the

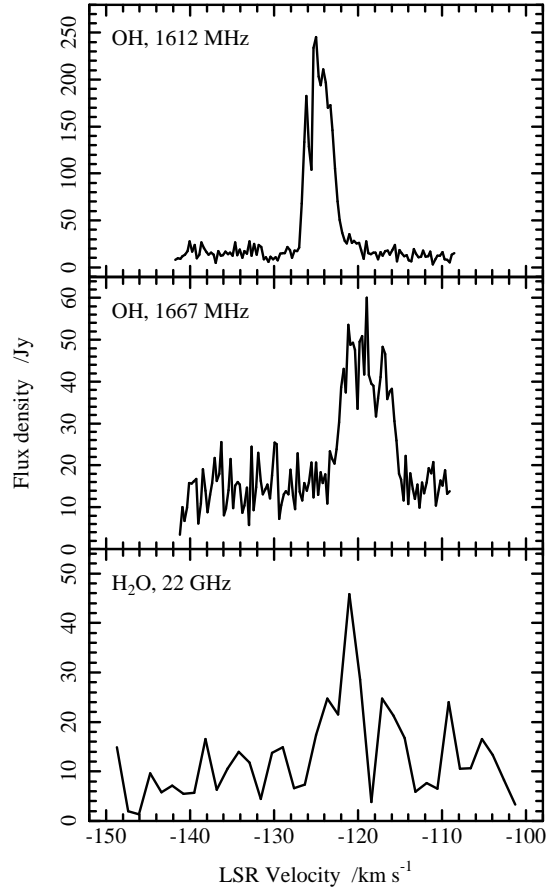


Figure 4. Masers observed towards H1–36 using the VLA in A configuration during 1994 May 01.

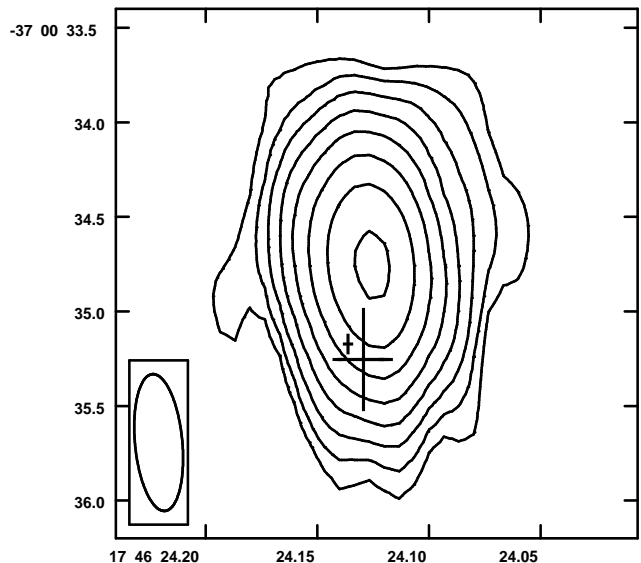


Figure 5. A-configuration 8.4-GHz isophotal map of H1–36 obtained during 1991 Sept). The positions of the OH and 22-GHz H₂O masers are marked and the size of the restoring beam is shown. Contours are plotted at 1, 2, 4 ... 128 times the $3\text{-}\sigma$ level of $0.25 \text{ mJy beam}^{-1}$.

Table 2. Parameters for the VLA A-configuration observations of H1–36 during 1994 May 01.

Line	Velocity resolution	Spectral noise (mJy)	Beamsize and PA (″ and °)	Central velocity	Integrated flux density (Jy km s ⁻¹)
OH – 1612 MHz	0.28 km s ⁻¹	5.2	2.2 × 0.6, 172	−124.5 ± 1.0 km s ⁻¹	0.71 ± 0.05
OH – 1667 MHz	0.27 km s ⁻¹	4.5	2.1 × 0.6, 172	−119 ± 1.0 km s ⁻¹	0.19 ± 0.03
H ₂ O – 22 GHz	1.32 km s ⁻¹	4.0	0.29 × 0.06, 22	−121 ± 1.5 km s ⁻¹	0.16 ± 0.04

lines, whilst the FWHM are ~ 4 and ~ 6 km s⁻¹ at 1612 and 1667 MHz, respectively. The velocity of the strongest peak at 1612 MHz corresponds with the 1993 May and July values (to within the uncertainties, Ivison et al. 1994). This is also true of the H₂O line (which is at only 25 per cent of its 1993 intensity).

If the observed 1612-MHz peak is the blueward component of the usual OH pair, then we can estimate a terminal wind velocity of 10 km s⁻¹ from its displacement from H1–36’s SiO and H92 α lines (Allen et al. 1989; Bastian 1992); furthermore, if the unseen redward peak has been obscured by optically thick, ionized gas (an idea first proposed by Allen et al. 1989 — see §5.2.3) then $\tau \geq 3.6$ at 1612 MHz, based on the spectral rms redward of the observed line.

5 ON THE R AQR SYSTEM

5.1 Radial velocity measurements in the radio

Several estimates of R Aqr’s orbital period have been proposed; none, however, have been robust. Table 3 lists the orbital periodicities that have been suggested to date, whilst more recent radial velocity (RV) data have been presented by Wallerstein (1986) and Hinkle et al. (1989). The RVs do not strongly support any of the suggested periodicities. Hinkle et al. state that the period must be between 18 and 21 yr or longer than 32 yr. Most solutions for periods of over 32 yr require $e > 0.3$.

Monitoring the position and velocity of the R Aqr water maser could reveal the system’s elusive binary period. The VLA offers both high velocity resolution and high positional accuracy with which to track a Mira. Table 1 shows the measurements from our first three epochs of monitoring; so far, there are no appreciable positional shifts and only one appreciable velocity shift. The problem could be that the timescale for the rise and fall of individual maser features (which is weakly correlated with the pulsational period) is shorter than the orbital period. This is compounded by strong, new maser features (such as that seen at the 0.4-Jy level in 1995 June) which can obscure weaker features such as the 0.1-Jy peak of 1994 May (see Fig. 1).

The 8-km s⁻¹ pedestal is the most enduring feature of the maser spectrum, and its stability at the $\Delta v_{\text{lsr}} < 1$ km s⁻¹ level over a period of two years implies a low orbital inclination, or a high $M_{\text{giant}} : M_{\text{dwarf}}$ ratio, or an orbital period that is measured in decades, which is consistent with optical data. If the pedestal is the result of thermal emission (at the 10-mJy level) from near the photosphere of the rotating LPV then its FWZM translates into a lower limit for the rotational period. The period will approach the lower limit if intrinsic line broadening is negligible, i.e. if the width is due entirely to Doppler broadening. The maximum photospheric

Table 3. Orbital periods suggested in the literature.

Periodicity /yr	Description
26.7	RV measurements (Merrill 1950). Later refuted by Jacobson & Wallerstein (1975).
24.7	Same RV data as Merrill (1950), used by Kurochkin (1976).
44	From two periods of peculiar activity in the Mira’s LC that are suggestive of its eclipse (Willson et al. 1981).

line-of-sight velocity implied by the pedestal is 4 km s⁻¹, well within the scatter of the observed rotational velocities for late-type giants ($v \sin i = 1 - 9$ km s⁻¹ for K giants, De Medeiros, Melo & Mayor 1996). This yields a rotational period of > 17 yr for an LPV radius of $500 \pm 100 R_{\odot}$ (Haniff, Scholz & Tuthill 1995; van Belle et al. 1996).

5.2 Mechanisms to explain the simultaneous data

5.2.1 Disruption by the white dwarf secondary?

Any periodicity in excess of 8 yr would yield a binary separation which would put the hot star in the H₂O maser zone (10–20 au), i.e., the companion star would orbit in the region normally occupied by the masing molecular gas. The companion could then reduce amplification by inducing turbulent motion and disrupting the velocity-coherent paths in the outer envelope where the bright 22-GHz masers form (Hall et al. 1990a, 1990b). The interaction of the accretion flow and the Mira’s wind could cause large velocity gradients and turbulence in the circumstellar envelope, which reduce the velocity coherence path (gain length).

5.2.2 Consistency with SIH95 model?

SIH95 put forward another model that appears to be consistent with the results of not only their survey of maser-line transitions towards symbiotic Miras, but also with the details of individual systems such as R Aqr and H1–36. In their model, UV radiation and a fast wind from the white dwarf companion dissociate and sweep away the dusty, molecular gas shed by the Mira. Even the molecular material shielded by the Mira from direct irradiation becomes dissociated as the result of Rayleigh scattering in the Mira’s wind. However, since the R Aqr hot component has a relatively low luminosity (and the nebula is ionisation bounded), the effectiveness of direct and indirect molecular dissociation by UV irradiation would be much reduced; even on the irradiated hemisphere of the Mira, an extensive neutral cavity

may remain beyond the ionization front of the hot dwarf. Thus we have an environment where 22-GHz H₂O masers may survive, in keeping with our observations.

The energy levels of the 22-GHz and 321-GHz transitions are 643 and 1861 K above the ground state, respectively. Yates, Field & Gray (1997) suggest that 321-GHz masers are excited closer to the Mira than 22-GHz masers. Given the absence of a suitable dusty, molecular environment in the outer reaches of the R Aqr Mira's wind, the observed 22-GHz H₂O maser lines will be weak and narrow in comparison to those observed towards field Miras.

Note also that our maps (Fig. 2) seem to indicate that the 22-GHz maser and the ionized gas are co-spatial (§3.1). This makes little sense unless the molecular gas is protected in a neutral cavity, much closer to the LPV than would normally be anticipated. The superimposition can be explained if the maser is within a cocoon of ionized gas and the strongest contribution to the free-free radiation component comes from the densest portion of the ionized wind, which is near the ionisation front and close to the Mira.

5.2.3 Line obscuration at low frequencies?

This was proposed Allen et al. (1989), and relies on the fact that the LPV's wind is optically thick at low frequencies. The spectral energy distributions of H1–36 and R Aqr show the turnover to optically thin free-free emission is at ~ 10 GHz (Ivison, Hughes & Bode 1992; Ivison et al. 1995b). Below 10 GHz, we can expect the line emission to be hidden from us by the optically thick, ionized gas.

The maser data support Allen's idea: first, the absence of OH maser emission towards R Aqr (see §3.3); second, only one component of the normal 1612-MHz OH mainline pair is seen towards H1–36, which suggests a large optical depth between the front and back of the masing shell in the line of sight through the system. Third, the observed lines become progressively more intense with increasing line frequency, suggesting lower obscuration: the OH line is absent, the 22-GHz emission is weak and the line emission at 43, 86, 299, 301 and 321 GHz is strong. There is no evidence, however, that the opacity at 22 GHz is sufficient to move the 22-/321-GHz line flux and luminosity ratios closer to those typically observed towards field Miras (a 22-/321-GHz line luminosity ratio of 1.5 would require $\tau \sim 2$ at 22 GHz).

6 CONCLUDING REMARKS

We have presented maser-line spectra and maps of the symbiotic Miras, R Aqr and H1–36, together with contemporaneous, high-resolution continuum maps. Our measurements have resulted in the first detection of sub-mm water maser emission towards a symbiotic system (R Aqr) and we have discussed three mechanisms that could cause the observed line properties in the geometries implied by the continuum and spectral-line maps.

With the data available to us, it is not possible to discriminate between three possible scenarios, although one of these requires conditions that are not supported by other measurements. The mechanisms that we favour inhibit the formation of OH and 22-GHz H₂O masers in their natural environments, employing either the orbital motion of the

companion or its radiation field and fast wind. The third, which reduces maser-line intensities via the free-free opacity of circumstellar, ionized gas (and thus has an effect that is dependent on the rest frequency of the maser transition) is somewhat less credulous since to reduce the intensity of the 22-GHz maser line by at least an order of magnitude relative to the 321-GHz line would require the free-free emission to remain optically thick at that frequency, which does not appear to be the case (see Ivison et al. 1992, 1995b).

REFERENCES

- Allen D.A., Hall P.J., Norris R.P., Troup E.R., Wark R.M., Wright A.E., 1989, MNRAS, 236, 363
 Bastian T.S., 1992, ApJ, 387, L77
 Bowers P., Hagen W., 1984, ApJ, 285, 637
 Chinarova L.L., Andronov I.L., Schweitzer E., 1996, in Proc. IAU Symp. No. 180. Kluwer, Dordrecht, in press
 De Medeiros J.R., Melo C.H.F., Mayor M., 1996, A&A, 309, 465
 Gray M.D., Ivison R.J., Humphreys E.M.L., Yates J.A., 1998, MNRAS, submitted
 Gray M.D., Ivison R.J., Yates J.A., Humphreys E.M.L., Hall P.J., Field D., 1995, MNRAS, 277, L67
 Hall P.J., Allen D.A., Troup E.R., Wark R.M., Wright A.E., 1990a, MNRAS, 243, 480
 Hall P.J., Wright A.E., Troup E.R., Wark R.M., Allen D.A., 1990b, MNRAS, 247, 549
 Haniff C.A., Scholz M., Tuthill P.G., 1995, MNRAS, 276, 640
 Hinkle K.H., Wilson T.D., Scharlach W.W.G., Fekel F.C., 1989, AJ, 98, 1820
 Hollis J.M., Wright M.C.H., Welch W.J., Jewell P.R., Crull Jr, H.E., Kafatos M., Michalitsianos A.G., 1990, ApJ, 361, 663
 Ivison R.J., Hughes D.H., Bode M.F., 1992, MNRAS, 257, 47
 Ivison R.J., Seaquist E.R., Hall P.J., 1994, MNRAS, 269, 218
 Ivison R.J., Seaquist E.R., Hall P.J., 1995a, in Watt G.D., Williams P.M., eds, Circumstellar Matter 1994, p. 255
 Ivison R.J., Seaquist E.R., Schwarz H.E., Hughes D.H., Bode M.F., 1995b, MNRAS, 273, 517
 Jacobson T.S., Wallerstein G., 1975, PASP, 87, 269
 Karovska M., Nisenson P., Beletic J., 1993, ApJ, 402, 311
 Kurochkin N.E., 1976, Soviet Astr. Lett., 2, 169
 Martinez A., Bujarrabal V., Alcolea J., 1988, A&A, 74, 273
 Menten K.M., Melnick G.J., 1991, ApJ, 377, 647
 Merrill P.W., 1950, ApJ, 112, 514
 Schwarz H.E., Nyman L.-Å., Seaquist E.R., Ivison, R.J., 1995, A&A, 303, 833
 Seaquist E.R., Krogulec M., Taylor A.R., 1993, ApJ, 410, 260
 Seaquist E.R., Ivison R.J., Hall P.J., 1995, MNRAS, 276, 867 (SIH95)
 Solf J., Ulrich H., 1985, A&A, 148, 274
 Sopka R.J., Herbig G., Kafatos M., Michalitsianos A.G., 1982, ApJ, 258, L35
 van Belle G.T., Dyck H.M., Benson J.A., Lacasse M.G., 1996, AJ, 112, 2147
 Wallerstein G., 1986, PASP, 98, 118
 Wallerstein G., Greenstein J.L., 1980, PASP, 92, 275
 Willson L.A., Garnavich P., Mattei J.A., 1981, Inf. Bull. Var. Stars, No. 1961
 Yates J.A., Cohen R.J., Hills R.E., 1995, MNRAS, 273, 529
 Yates J.A., Field D., Gray M.D., 1997, MNRAS, 285, 303

This paper has been produced using the Royal Astronomical Society/Blackwell Science L^AT_EX style file.